THE UNIVERSITY *of* EDINBURGH

Edinburgh Research Explorer

ADAPTIVE OPTICS IMAGING OF VHS 1256-1257: A LOW MASS COMPANION TO A BROWN DWARF BINARY SYSTEM

OPEN ACCESS

ADAPTIVE OPTICS IMAGING OF VHS 1256-1257: A LOW MASS COMPANION TO A BROWN DWARF BINARY SYSTEM

Jordan M. Stone[1], Andrew J. Skemer[1,2], Kaitlin M. Kratter[1], Trent J. Dupuy[3], Laird M. Close[1], Josh A. Eisner[1], Jonathan J. Fortney[2], Philip M. Hinz[1], Jared R. Males[1], Caroline V. Morley[2], Katie M. Morzinski[1], and Kimberly Ward-Duong[4]
Draft version September 24, 2018

ABSTRACT

Recently, Gauza et al. (2015) reported the discovery of a companion to the late M-dwarf, VHS J125601.92-125723.9 (VHS 1256-1257). The companion's absolute photometry suggests its mass and atmosphere are similar to the HR 8799 planets. However, as a wide companion to a late-type star, it is more accessible to spectroscopic characterization. We discovered that the primary of this system is an equal-magnitude binary. For an age ~ 300 Myr the A and B components each have a mass of $64.6^{+0.8}_{-2.0}$ $M_{\rm Jup}$, and the b component has a mass of $11.2^{+9.7}_{-1.8}$, making VHS 1256-1257 only the third brown dwarf triple system. There exists some tension between the spectrophotometric distance of 17.2 ± 2.6 pc and the parallax distance of 12.7 ± 1.0 pc. At 12.7 pc VHS 1256-1257 A and B would be the faintest known M7.5 objects, and are even faint outliers among M8 types. If the larger spectrophotmetric distance is more accurate than the parallax, then the mass of each component increases. In particular, the mass of the b component increases well above the deuterium burning limit to ~ 35 $M_{\rm Jup}$ and the mass of each binary component increases to 73^{+20}_{-17} $M_{\rm Jup}$. At 17.1 pc, the UVW kinematics of the system are consistent with membership in the AB Dor moving group. The architecture of the system resembles a hierarchical stellar multiple suggesting it formed via an extension of the star-formation process to low masses. Continued astrometric monitoring will resolve this distance uncertainty and will provide dynamical masses for a new benchmark system.

1. INTRODUCTION

Brown dwarfs in the field follow a tight sequence in near-infrared color magnitude diagrams (e.g., Dupuy & Liu 2012). At the hottest and most massive end, M-type dwarfs transition to L-type dwarfs as they cool. L-dwarfs are characterized by red color and thick clouds with CO as the dominant carrier of atmospheric carbon. At $T_{\rm eff} \sim 1300$ K, the L-dwarfs undergo a dramatic transition to T-type, becoming relatively cloud free, bluer, and methane dominated.

In the last few years, a growing population of objects at effective temperatures where field brown dwarfs are seen to be T-type, are instead observed to be L-type, suggesting an extension of the L-dwarf sequence to low temperature (Figure 1). These objects include the four directly imaged planets in the HR 8799 system (Marois et al. 2008, 2010), the planetary mass binary companion 2MASS 1207 b (Chauvin et al. 2004), and free floating brown dwarfs such as the planetary mass PSO J318.5-22 (Liu et al. 2013). The common characteristic of these objects is low gravity due to low mass and young age.

A recently discovered companion, VHS J125601.92-125723.9 b (hereafter VHS 1256-1257 b, $d = 12.7$ pc, $M \sim 11 M_{\rm Jup}$, age 150–300 Myr; Gauza et al. 2015), is

thought to be one of the most extreme members of the extension to the L-dwarf sequence (Figure 1). It appears in many ways to be an analogue of HR 8799 b, the faintest and least massive planet in the HR 8799 system. This discovery is significant because VHS 1256-1257 b is substantially easier to observe than HR 8799 b as it orbits a fainter host at larger separation. This means that more precise measurements can be made with a wider array of instruments because issues with high contrast are alleviated.

The variety of objects that occupy the extended L-dwarf region in color-magnitude diagrams suggests that distinguishing planets, which form via accumulation of material in a circumstellar disk (e.g., Sallum et al. 2015), from brown dwarfs, which form as an extension of the star-formation process to low masses (e.g., Chabrier et al. 2014), requires some care; additional constraints such as compositional differences (e.g., Skemer et al. 2015), or system architecture (e.g., Lodato et al. 2005) must be incorporated into the analysis.

In this letter we present evidence that the host of VHS 1256-1257 b is actually a 0.1″ equal-mass brown dwarf binary system and discuss the implications for the nature of this system[5].

2. OBSERVATIONS AND RESULTS

2.1. *MagAO/Clio2 L'*

On 2015 June 4 UT, we imaged the VHS 1256-1257 system (all components simultaneously) with MagAO/Clio2 (Sivanandam et al. 2006; Hinz et al. 2010; Close et al.

[1] Steward Observatory, University of Arizona, 933 N. Cherry Ave, Tucson, AZ 85721-0065 USA
[2] Department of Astronomy and Astrophysics, University of California, Santa Cruz, 1156 High St, Santa Cruz, CA 95064, USA
[3] The University of Texas at Austin, Department of Astronomy, 2515 Speedway C1400, Austin, TX 78712, USA
[4] School of Earth and Space Exploration, Arizona State University, Tempe, AZ, 85287, USA

[5] Note added in proof: independant ao-images presented by Rich et al., in prep
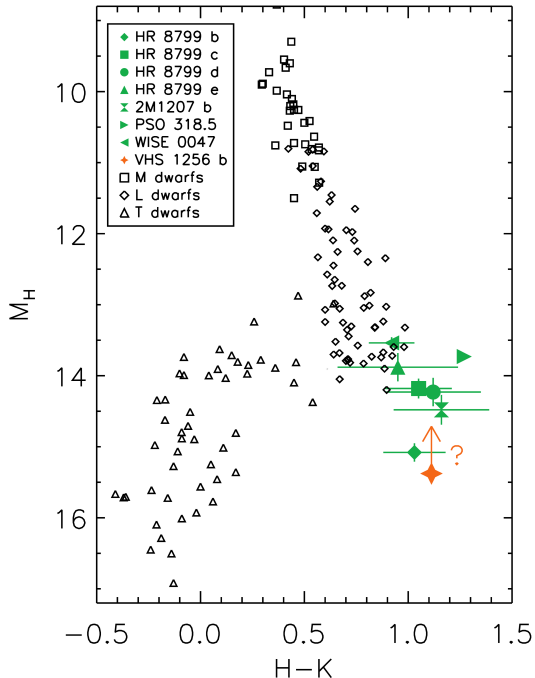
Figure 1. Near-infrared color magnitude diagram. The field brown dwarf sequence is shown with open symbols (data from Dupuy & Liu 2012). The L to T transition begins at $M_H \sim 14$. We also plot, with green filled symbols, the planets in the HR 8799 system (data compiled from Marois et al. 2008; Metchev et al. 2009; Marois et al. 2010; Skemer et al. 2012), the planetary mass companion 2M 1207 b ($M \sim 8\ M_{\rm Jup}$, Chauvin et al. 2004), and the free-floating object PSO J318.5 (Liu et al. 2013). With an orange star we show VHS 1256-1257 b, which appears furthest from the field-dwarf sequence. The binary nature of its host may imply a larger distance to the system which would push VHS 1256-1257 b up in the diagram.

2013) as part of a campaign to characterize the atmospheres of low-gravity cool companions to nearby stars. The PSF of the primary appeared extended compared to brighter point-sources observed the same night.

Our images were obtained as acquisition images for a spectroscopic observation, so they were not optimized for highest spatial resolution. We observed in coarse platescale mode (27.477 ± 0.085 mas pixels^{-1}; Morzinski et al. 2015) through the L' filter. We used 0.28 s integrations to keep the bright sky emission in the linear range of the detector. Files were written with five coadded frames each. We nodded the telescope in an AB pattern, saving ten files per position. From each of the ten images per nod, we subtracted the median of the ten frames from the opposite nod position. This corrects for the bright sky emission, dark current, and the detector bias.

We measured the flux ratio, separation, and position angle of the marginally-resolved binary components in each of our images by fitting a two-component model created using an image of HIP 57173 —an unresolved star— as a template PSF. Our fitting procedure optimized 6-parameters including an amplitude and an (x, y) position for each source. The best-fit model gave a magnitude difference of 0.07 ± 0.03 a separation of 109 ± 1.8 milliarcseconds and a PA of $173^\circ\!.3 \pm 0^\circ\!.9$. Errorbars were

derived by bootstrapping the final stack of background subtracted images. All of our deduced binary parameters are reported in Table 1. Our final stacked image is shown in Figure 2.

2.2. *Keck NIRC2 J, H, Ks*

To confirm the binary nature of VHS 1256-1257 AB we conducted follow-up imaging with a larger aperture and at shorter wavelengths to achieve better spatial resolution. We used natural-guidestar adaptive optics (Wizinowich et al. 2000) and the NIRC2 instrument on the Keck II telescope on 2015 November 29 UT. Data were collected through the J, H, and Ks filters, and the camera was set up in the 9 mas pixel^{-1} mode. We used a three-point dither pattern in order to track variable sky background. Files were saved using three coadds of five second exposures. We obtained a total of 45 s of open shutter time per filter.

We reduced and analyzed our NIRC2 images in the same fashion as in previous work (e.g., see Dupuy et al. 2009, 2015). For each individual image, we applied standard calibrations (dark subtraction, flat fielding) and then fit an analytic, three-component Gaussian model to both objects simultaneously. To convert the raw (x, y) coordinates from these fits to separation and position angle (PA) on the sky, we applied the nonlinear distortion solution of (Yelda et al. 2010) and their corresponding pixel scale of 9.952 ± 0.002 mas pixel^{-1} and NIRC2 header orientation correction of $+0^\circ\!.252 \pm 0^\circ\!.009$. In Table 1 we report the mean and rms of the binary parameters we derived from our individual images. The separation measurements across JHK_S bands are in good agreement within the quoted uncertainties, but the PA values do not agree within their much smaller quoted uncertainties. Since the binary components have nearly identical fluxes and colors, this is unlikely to be due to a chromatic effect, but it could be caused by recent changes to the nonlinear distortion of NIRC2 (J. Lu, 2015 private communication). We therefore adopt the mean and rms of the separations and PAs determined across JHK_S bands as the final values, 123.6 ± 0.4 mas and $170^\circ\!.2 \pm 0^\circ\!.6$, respectively.

We also briefly observed the outer tertiary component, VHS 1256-1257 b. We obtained three frames in three separate nod positions— one of which contained all three components at the same time. An exposure of 60 seconds was collected for each nod. We reduced these images as explained above. The object appears single down to our sensitivity. We see no equal magnitude component down to ~ 70 mas and no component 1 magnitude fainter down to ~ 100 mas. We cannot rule out companions more than 2 magnitudes fainter than VHS 1256-1257 b.

2.3. *Ruling Out the Background Hypothesis*

To confirm that the binary components are physically related and not the result of a chance alignment, we inspected 2MASS images from 1999 March 1 UT. We see no source at the present-day location of VHS 1256-1257 AB, and no sources with the correct magnitude within 2 arcminutes. Given the high proper motion of the system (~ 300 mas yr^{-1}) this strongly suggests the pair is a common proper motion binary and is physically bound.

3. DISCUSSION AND ANALYSIS

Table 1
Binary Properties

Date [UT]	Filter	Flux Ratio [mag]	Separation [mas]	PA [°]	m_A [a] [mag]	m_B [a] [mag]	d_L [b] [pc]
2015 Nov 29	J	0.05 ± 0.04	123.1 ± 1.0	170.8 ± 0.2	11.76 ± 0.05	11.78 ± 0.05	16.8 ± 2.4
2015 Nov 29	H	0.04 ± 0.02	123.8 ± 0.4	170.1 ± 0.1	11.21 ± 0.05	11.24 ± 0.05	17.4 ± 2.6
2015 Nov 29	Ks	0.04 ± 0.03	123.9 ± 0.5	169.6 ± 0.1	10.79 ± 0.04	10.81 ± 0.04	17.2 ± 2.6
2015 Jun 03	L'	0.07 ± 0.03	109.4 ± 0.9	173.3 ± 0.9	$\cdots$	$\cdots$	$\cdots$

[a] Individual magnitudes determined using 2MASS unresolved photometry and our flux ratio. We assume the J- and H-band flux ratios we measure in the MKO system will be the same in the 2MASS system given the similar spectral types of each component implied by the flux ratio being so close to one.
[b] Spectrophotometric distance implied by M7.5 spectral type. Uncertainty includes contributions from measurement errors and the rms variation in the population of well characterized sources in Dupuy & Liu (2012).
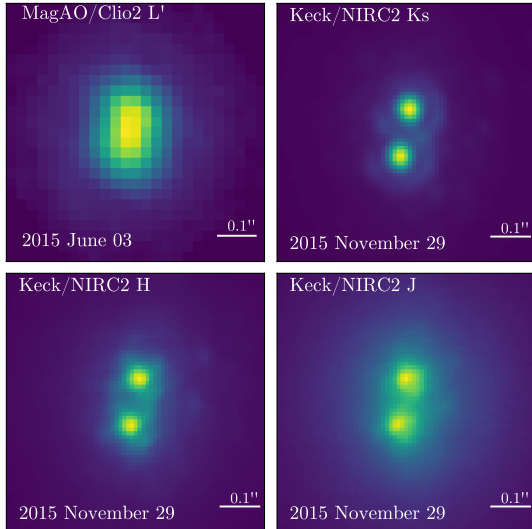

Figure 2. Images of the central binary in the VHS 1256-1257 system. North is up, and East is Left. The cool companion is 8" to the southwest, off the frame.

Figure 3. Near-infrared color magnitude diagram of late-M type objects in the field. Data taken from Dupuy & Liu (2012) show the average and rms spread for each spectral type. We also show VHS 1256-1257 A and B (both spectroscopically determined to be M7.5±0.5) with the absolute magnitude implied given the distance of 12.7 pc reported by Gauza et al. (2015). VHS 1256-1257 A and B are more than 2-σ less luminous than average field M7.5 objects and are 1-σ less luminous than typical M8s. The tension with expectations is amplified by the age of the system because young objects like VHS 1256-1257 are expected to be more luminous than field objects, not less.

3.1. Distance and Luminosity

Gauza et al. (2015) report a parallax distance to VHS 1256-1257 of 12.7 ± 1 pc using $\sim$ 9 months of astrometric monitoring data —collected in a variety of filters— together with a 2MASS point. This distance was consistent with the spectrophotometric distance of the central source, given the spectroscopically determined type of M7.5±0.5 (Gauza et al. 2015), assuming that it was a single star with typical absolute magnitude (averages taken for field objects from Dupuy & Liu 2012). However, the fact that the source is an equal magnitude binary, not a single star, requires a reexamination of the spectrophotometric distance. An equal magnitude binary will be 0.75 magnitudes brighter and the derived spectrophotometric distance will scale by a factor of $\sqrt{2}$. In Table 1, we show the implied spectrophotometric distance of VHS 1256-1257 from the apparent magnitudes of the resolved components. We use the average and rms scatter for M7.5 spectral type objects with precise parallax measurements from Dupuy & Liu (2012). The distances derived from each band are consistent with each other and suggest that the system is located at $\sim 17.1 \pm 2.5$ pc, with the uncertainty dominated by the rms variation in absolute magnitude of the population.

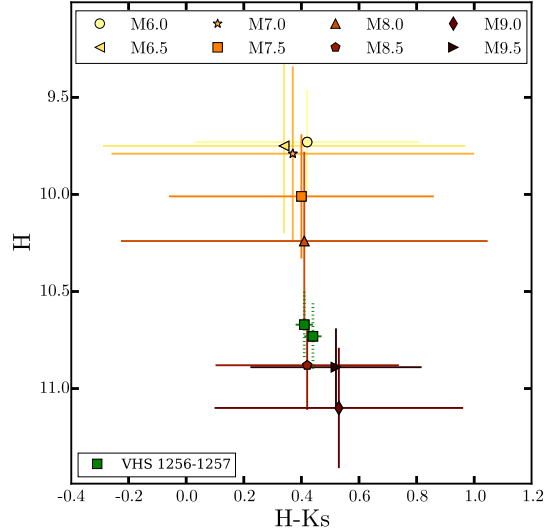In this case, the distance modulus to VHS 1256-1257

increases by 0.66 mags and components move up in color magnitude-diagrams. In particular, the planetary mass companion would appear more like the hotter, more-massive HR 8799 d than HR 8799 b (Figure 1). Furthermore, a higher luminosity for VHS 1256-1257 b also implies a higher mass —up to 35 M_{Jup} (for 300 Myr, $M_{Ks} = 13.38$; Baraffe et al. 2015)— placing it above the deuterium burning limit.

The UVW kinematics of the system also change if it is located at 17.1 pc. While Gauza et al. (2015) show that the UVW velocities of VHS 1256-1257 are consistent with the β Pic moving group, they argue that it cannot be a member due to the lack of lithium and the much older age. We made use of BANYAN II tool (Malo et al. 2013; Gagné et al. 2014) to determine the probability that the system is a member of nearby moving groups. We indicated that VHS 1256-1257 is less than 1 Gyr old based on the very-low gravity designation of the b component. At a distance of 17.1 pc the BANYAN II predicts mem-
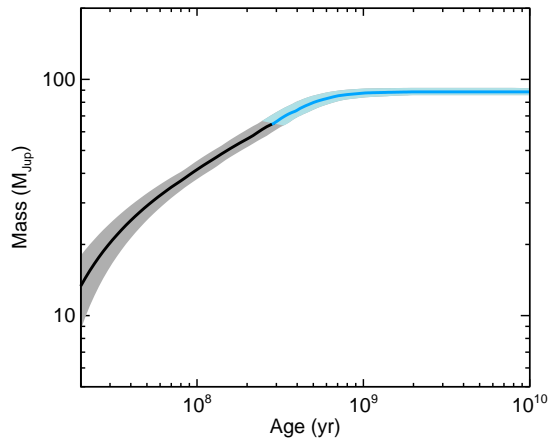
Figure 4. Age versus mass at constant luminosity according to the evolutionary model grid of Chabrier et al. (2000). We assume the luminosity of each binary component if the parallax distance reported by Gauza et al. (2015) is correct. The width of the curve accommodates the uncertainty in the luminosity from our reported photometric errors and the error in the distance measurement. We highlight in blue models with less than 10% of the primordial lithium abundance, which are consistent with the non-detection from Gauza et al. (2015).

bership in the older AB Dor moving group with 66.85% probability, membership in the young field population with a 32.52% probability, and membership in the β Pic moving group of 0.48%.

This scenario requires the parallax for the system to be less precise than reported, possibly due to the inhomogeneous nature of the astrometric data and the small number of epochs used to disentangle the parallax motion from the proper motion. Alternatively, the parallax distance is correct and the absolute magnitude of the binary components are intrinsically quite low.

In Figure 3, we show the average and rms spread in absolute H-band magnitude and H-Ks color for late-M field brown dwarfs (data from Dupuy & Liu 2012). VHS 1256-1257 A and B lie well below the average M7.5 point by more than 2 σ. The uncertainty in the spectral type of the VHS 1256-1257 A and B does accommodate a fainter M8 spectral type. Even for this spectral type the binary components are less luminous than expected, yet are near the edge of the rms scatter in the well characterized field population. At Ks band, if the system is at 12.7 pc, VHS 1256-1257 A and B are the least luminous M7.5 objects known with $M_{Ks} = 10.26 \pm 0.18$. GRH 2208-20, an M7.5 object, has $M_{Ks} = 10.11 \pm 0.06$, all other M7.5 sources with precise parallax have $M_{Ks} < 10$ (Dupuy & Liu 2012). Even among M8 types, at 12.7 pc VHS 1256-1257 A and B are faint. The only other M8 with an absolute K-band luminosity greater than 10 is LHS 2397a A ($M_{Ks} = 10.13 \pm 0.07$).

Such low luminosities are odd given age constraints inferred from the INT-G and VL-G gravity designations given to the unresolved binary and the companion (age < 500 Myr; Gauza et al. 2015). Young low-gravity objects are expected to be more luminous than field objects based on theoretical evolution models and observations of young populations (e.g., Casewell et al. 2007; Baraffe et al. 2015). However, the number of well characterized INT-G M7-8 objects with which to compare our measured absolute magnitudes is small, making it

difficult to rule out the low-luminosity explanation.

3.2. *Mass and Orbital Period*

If the parallax distance is correct, then the mass of the binary components need to be updated. Using the evolutionary models of Chabrier et al. (2000) we construct a plot of age versus mass at constant luminosity (Figure 4). We assume a luminosity for each source of $log(\frac{L}{L_\odot}) = -3.44 \pm 0.1$, half that reported by Gauza et al. (2015). Since the objects have no detectable lithium (Gauza et al. 2015), we indicate in Figure 4 those models which have less than 10% of the primordial lithium abundance by coloring them blue. The minimum mass for each of the binary components is $64.6^{+0.8}_{-2.0}$ M_{Jup} and the corresponding minimum age is 280^{+40}_{-50} Myr.

Using our new mass estimate, we can calculate an orbital period for VHS 1256-1257 A and B. To do this, we take the projected separation measured in our discovery image and correct it using the projected separation–semi-major axis correction factor for a moderate discovery bias (due to the close separation of the binary) taken from Dupuy & Liu (2011a). We find an orbital period of 5.87 ± 2.7 yr. If the system is located at 17.1 pc, as suggested by the photometry of the components, then the period changes because the projected separation increases as does the mass of each component. In this case, the orbital period is 8.7 ± 4.3 yr. Given these orbital periods and our observation of $\lesssim 3°$ of change in the PA of the binary components, the binary orbit cannot be face-on and circular.

3.3. *Formation and Dynamical Evolution*

We have shown that VHS 1256-1257 consists of three brown dwarf objects organized into a hierarchical triple system, the A and B components being orbited by the more distant b component. Only two other brown dwarf triples appear in the literature, 2MASS J08381155+1511155 (composed of three T-dwarfs; Radigan et al. 2013), and DENIS-P J020529.0-115925 (marginally resolved late-L and early T components; Bouy et al. 2005). Neither includes M-type objects nor a planetary mass component. 2M0441+2301 AabBab (Todorov et al. 2010; Bowler & Hillenbrand 2015) includes three substellar components including one below the deuterium burning limit, yet the system also includes a stellar component and the hierarchical quadruple architecture is much different from VHS 1256-1257. VHS 1256-1257 shares many characteristics with 2MASS J01033563-5515561(AB)b, a hierarchical triple with a planetary mass companion orbiting a binary composed of M6-type stars (Delorme et al. 2013). However, VHS 1256-1257 is closer, older, and less massive.

The hierarchical-triple orbital configuration of VHS 1256-1257 suggests that the system is more akin to a low mass analog of a stellar multiple, rather than a planetary system with a planet on a wide orbit. Models for turbulent fragmentation suggest that isolated objects may form at masses more than a factor of two below VHS 1256-1257 b (Hennebelle & Chabrier 2008). The separation of VHS 1256-1257 AB is consistent with the sample of brown dwarf binaries observed by Close et al. (2003) and Dupuy & Liu (2011b), who showed that low mass binaries typically have smaller semi-major

axes than their stellar counterparts. These scaled down separations are expected if brown dwarfs form as a low mass tail of the turbulent core fragmentation process Jumper & Fisher (2013). The presence of a high mass ratio (∼10%) tertiary at relatively wide separations is similarly consistent with low mass star formation (Reipurth & Clarke 2001; Offner et al. 2010; Bate 2012). If the three objects formed from the same filament, the objects could have undergone early dynamical interactions which naturally tighten one orbit in exchange for softening the outer most orbit (Heggie 1975; Reipurth & Mikkola 2015). We suggest early dynamical interactions are the most likely origin for the orbital configuration due to low stellar densities in the solar neighborhood. Although mutual inclination between the two orbits could induce Kozai-Lidov oscillation on Myr timescales, the inner orbit is too wide to undergo significant tidal evolution over the lifetime of the system (Fabrycky & Tremaine 2007).

4. CONCLUSION

We have revealed that the host of VHS 1256-1257 b is actually an equal-mass brown dwarf binary, making VHS 1156-1257 the third triple system known with exclusively substellar components. There is some tension between the parallax distance and the spectrophotometric distance to the system. This implies that either the system is more distant than reported, and the planetary mass companion more massive ($\sim 35\ M_{\rm Jup}$ for an age of 300 Myr) or the components are less luminous than expected based on their age and spectral type. The architecture of this system is consistent with outcomes from normal low-mass star formation. Continued astrometric monitoring of this system will resolve the tension between the luminosity and parallax distances, and enable dynamical mass measurements for the components, providing important benchmarks for these low-gravity objects.

REFERENCES

Baraffe, I., Homeier, D., Allard, F., & Chabrier, G. 2015, A&A, 577, A42

Bate, M. R. 2012, MNRAS, 419, 3115

Bouy, H., Martín, E. L., Brandner, W., & Bouvier, J. 2005, AJ, 129, 511

Bowler, B. P. & Hillenbrand, L. A. 2015, ApJ, 811, L30

Casewell, S. L., Dobbie, P. D., Hodgkin, S. T., Moraux, E., Jameson, R. F., Hambly, N. C., Irwin, J., & Lodieu, N. 2007, MNRAS, 378, 1131

Chabrier, G., Baraffe, I., Allard, F., & Hauschildt, P. 2000, ApJ, 542, 464

Chabrier, G., Johansen, A., Janson, M., & Rafikov, R. 2014, Protostars and Planets VI, 619

Chauvin, G., Lagrange, A.-M., Dumas, C., Zuckerman, B., Mouillet, D., Song, I., Beuzit, J.-L., & Lowrance, P. 2004, A&A, 425, L29

Close, L. M., Males, J. R., Morzinski, K., Kopon, D., Follette, K., Rodigas, T. J., Hinz, P., Wu, Y.-L., Puglisi, A., Esposito, S., Riccardi, A., Pinna, E., Xompero, M., Briguglio, R., Uomoto, A., & Hare, T. 2013, ApJ, 774, 94

Close, L. M., Siegler, N., Freed, M., & Biller, B. 2003, ApJ, 587, 407

Delorme, P., Gagné, J., Girard, J. H., Lagrange, A. M., Chauvin, G., Naud, M.-E., Lafrenière, D., Doyon, R., Riedel, A., Bonnefoy, M., & Malo, L. 2013, A&A, 553, L5

Dupuy, T. J., Kratter, K. M., Kraus, A. L., Isaacson, H., Mann, A. W., Ireland, M. J., Howard, A. W., & Huber, D. 2015, ArXiv e-prints

Dupuy, T. J. & Liu, M. C. 2011a, ApJ, 733, 122

—. 2011b, ApJ, 733, 122

—. 2012, ApJS, 201, 19

Dupuy, T. J., Liu, M. C., & Bowler, B. P. 2009, ApJ, 706, 328

Fabrycky, D. & Tremaine, S. 2007, ApJ, 669, 1298

Gagné, J., Lafrenière, D., Doyon, R., Malo, L., & Artigau, É. 2014, ApJ, 783, 121

Gauza, B., Béjar, V. J. S., Pérez-Garrido, A., Rosa Zapatero Osorio, M., Lodieu, N., Rebolo, R., Pallé, E., & Nowak, G. 2015, ApJ, 804, 96

Heggie, D. C. 1975, MNRAS, 173, 729

Hennebelle, P. & Chabrier, G. 2008, ApJ, 684, 395

Hinz, P. M., Rodigas, T. J., Kenworthy, M. A., Sivanandam, S., Heinze, A. N., Mamajek, E. E., & Meyer, M. R. 2010, ApJ, 716, 417

Jumper, P. H. & Fisher, R. T. 2013, ApJ, 769, 9

Liu, M. C., Magnier, E. A., Deacon, N. R., Allers, K. N., Dupuy, T. J., Kotson, M. C., Aller, K. M., Burgett, W. S., Chambers, K. C., Draper, P. W., Hodapp, K. W., Jedicke, R., Kaiser, N., Kudritzki, R.-P., Metcalfe, N., Morgan, J. S., Price, P. A., Tonry, J. L., & Wainscoat, R. J. 2013, ApJ, 777, L20

Lodato, G., Delgado-Donate, E., & Clarke, C. J. 2005, MNRAS, 364, L91

Malo, L., Doyon, R., Lafrenière, D., Artigau, É., Gagné, J., Baron, F., & Riedel, A. 2013, ApJ, 762, 88

Marois, C., Macintosh, B., Barman, T., Zuckerman, B., Song, I., Patience, J., Lafrenière, D., & Doyon, R. 2008, Science, 322, 1348

Marois, C., Zuckerman, B., Konopacky, Q. M., Macintosh, B., & Barman, T. 2010, Nature, 468, 1080

Metchev, S., Marois, C., & Zuckerman, B. 2009, ApJ, 705, L204

Morzinski, K. M., Males, J. R., Skemer, A. J., Close, L. M., Hinz, P. M., Rodigas, T. J., Puglisi, A., Esposito, S., Riccardi, A., Pinna, E., Xompero, M., Briguglio, R., Bailey, V. P., Follette, K. B., Kopon, D., Weinberger, A. J., & Wu, Y.-L. 2015, ArXiv e-prints

Offner, S. S. R., Kratter, K. M., Matzner, C. D., Krumholz, M. R., & Klein, R. I. 2010, ApJ, 725, 1485

Radigan, J., Jayawardhana, R., Lafrenière, D., Dupuy, T. J., Liu, M. C., & Scholz, A. 2013, ApJ, 778, 36

Reipurth, B. & Clarke, C. 2001, AJ, 122, 432

Reipurth, B. & Mikkola, S. 2015, AJ, 149, 145

Sallum, S., Follette, K. B., Eisner, J. A., Close, L. M., Hinz, P., Kratter, K., Males, J., Skemer, A., Macintosh, B., Tuthill, P., Bailey, V., Defrère, D., Morzinski, K., Rodigas, T., Spalding, E., Vaz, A., & Weinberger, A. J. 2015, Nature, 527, 342

Sivanandam, S., Hinz, P. M., Heinze, A. N., Freed, M., &
    Breuninger, A. H. 2006, in Society of Photo-Optical
    Instrumentation Engineers (SPIE) Conference Series, Vol. 6269,
    Society of Photo-Optical Instrumentation Engineers (SPIE)
    Conference Series, 0

Skemer, A. J., Hinz, P. M., Esposito, S., Burrows, A., Leisenring,
    J., Skrutskie, M., Desidera, S., Mesa, D., Arcidiacono, C.,
    Mannucci, F., Rodigas, T. J., Close, L., McCarthy, D., Kulesa,
    C., Agapito, G., Apai, D., Argomedo, J., Bailey, V., Boutsia,
    K., Briguglio, R., Brusa, G., Busoni, L., Claudi, R., Eisner, J.,
    Fini, L., Follette, K. B., Garnavich, P., Gratton, R., Guerra,
    J. C., Hill, J. M., Hoffmann, W. F., Jones, T., Krejny, M.,
    Males, J., Masciadri, E., Meyer, M. R., Miller, D. L.,
    Morzinski, K., Nelson, M., Pinna, E., Puglisi, A., Quanz, S. P.,
    Quiros-Pacheco, F., Riccardi, A., Stefanini, P., Vaitheeswaran,
    V., Wilson, J. C., & Xompero, M. 2012, ApJ, 753, 14

Skemer, A. J., Morley, C. V., Zimmerman, N. T., Skrutskie,
    M. F., Leisenring, J., Buenzli, E., Bonnefoy, M., Bailey, V.,
    Hinz, P., Defrére, D., Esposito, S., Apai, D., Biller, B.,
    Brandner, W., Close, L., Crepp, J. R., De Rosa, R. J.,
    Desidera, S., Eisner, J., Fortney, J., Freedman, R., Henning, T.,
    Hofmann, K.-H., Kopytova, T., Lupu, R., Maire, A.-L., Males,
    J. R., Marley, M., Morzinski, K., Oza, A., Patience, J., Rajan,
    A., Rieke, G., Schertl, D., Schlieder, J., Stone, J., Su, K., Vaz,
    A., Visscher, C., Ward-Duong, K., Weigelt, G., & Woodward,
    C. E. 2015, ArXiv e-prints

Todorov, K., Luhman, K. L., & McLeod, K. K. 2010, ApJ, 714,
    L84

Wizinowich, P., Acton, D. S., Shelton, C., Stomski, P., Gathright,
    J., Ho, K., Lupton, W., Tsubota, K., Lai, O., Max, C., Brase,
    J., An, J., Avicola, K., Olivier, S., Gavel, D., Macintosh, B.,
    Ghez, A., & Larkin, J. 2000, PASP, 112, 315

Yelda, S., Lu, J. R., Ghez, A. M., Clarkson, W., Anderson, J.,
    Do, T., & Matthews, K. 2010, ApJ, 725, 331